International Journal of Engineering & Technology, 4 (4) (2015) 531-537
www.sciencepubco.com/index.php/IJET
©Science Publishing Corporation
doi: 10.14419/ijet.v4i4.5139
Research Paper

Selection of window for inter-pulse analysis of simple pulsed radar signal using the short time Fourier transform

Ashraf Adamu Ahmad *, Abdullahi Daniyan, David Ocholi Gabriel

Department of Electrical and Electronic Engineering, Federal University of Technology, PMB 65, Minna, Nigeria
**Corresponding author E-mail: saintashraf@gmail.com*

Copyright © 2015 Ashraf Adamu Ahmad et al. This is an open access article distributed under the Creative Commons Attribution License, which permits unrestricted use, distribution, and reproduction in any medium, provided the original work is properly cited.

Abstract

The electronic intelligence (ELINT) system is used by the military to detect, extract information and classify incoming radar signals. This work utilizes short time Fourier transform (STFT) - time frequency distribution (TFD) for inter-pulse analysis of the radar signal in order to estimate basic radar signal time parameters (pulse width and pulse repetition period). Four well-known windows functions of different and unique characteristics were used for the localization of STFT to determine their various effects on the analysis. The window functions are Hamming, Hanning, Bartlett and Blackman window functions. Monte Carlo simulation is carried out to determine the performance of the signal analysis in presence of additive white Gaussian noise (AWGN). Results show that the lower the transition of main lobe width and higher the peak side lobe, the better the performance of the window function irrespective of time parameter being estimated. This is because 100 percent probability of correct estimation is achieved at signal to noise ratio of about -2dB for Bartlett, 4dB for both Hamming and Hanning, and 9dB for Blackman.

Keywords: *Additive White Gaussian Noise (AWGN); Airborne Radar; Electronic Warfare; Signal Analysis; Signal to Noise Ratio.*

1. Introduction

Electronic warfare is the art and science of preserving the use of the electromagnetic spectrum for friendly use while denying its use to the enemy [1] [2]. It employs the use of radar, an electromagnetic sensor that detects the position of an object in space to extract relevant information or to attack a given target via electronic means. The electronic warfare is subdivided into three branches- the Electronic-Counter Counter Measures (ECCM), the Electronic Counter Measures (ECM) and the Electronic Support Measures (ESM). The field of Electronic Intelligence (ELINT) for which this paper finds application in, is a major aspect of the ECCM. ELINT is the process of analysing radar signals in order to obtain information pertaining to these signals [3].

The radar signal has two main basic time characteristics; the time in which the radar system radiates each pulse (the pulse width (PW)) and the time between the beginning of one pulse and the start of the next pulse (the pulse repetition period (PRP)). The inter-pulse analysis is used to determine the value of these time parameters and from which range resolution, theoretical unambiguous range and angle of target among other functions can be determined [3][4]. The time-frequency (T-F) analysis has been identified as a key signal processing tool for inter-pulse analysis, and in this case, the classical and linear but still very much in use short time Fourier transform (STFT) is utilized. Recently in the field of radar signal processing, the STFT has been used in conjunction with fractional Fourier transform (FrFT) for micro-Doppler (m-D) signal removal [5], instantaneous frequency (IF) and direction pattern algorithm for m-D signal estimation [6], independent sub-space analysis (ISA) for narrow-band interference (NBI) mitigation [7], IF and autocorrelation function for classification of airborne radar signal types [8] to mention a few.

This paper provides an alternative algorithm based on STFT and its resulting peak to accurately determine the pulse width (PW) and pulse repetition period (PRP) in the presence of additive white Gaussian noise (AWGN), while also presenting the effect of the window functions (Hamming, Hanning, Bartlett and Blackman) on the analysis. The rest of the paper is as follows; section 2 presents the important literatures and theories associated with the method used such as

the STFT and the window functions, the methodology of the algorithm is presented in section 3 while results and discussion are shown in section 4. Finally, the paper ends with the conclusive remarks.

2. Literature review

Signals in monostatic radars are generated using oscillators and transmitted to the duplexer. The duplexer switches the antenna mode to either receiving or transmitting. The antenna propagates this signal to space, which is received by the antenna after being reflected by the target but with a lesser power than that actually transmitted from the antenna [9]. For ELINT applications, this signal is then de-interleaved and demodulated, thereafter signal processing tools are then used to obtain relevant parameters such as PW, PRP, range, velocity, etc. The common simple pulsed radar signal of constant PRP and of no pulse compression capability is illustrated in Fig. 1.

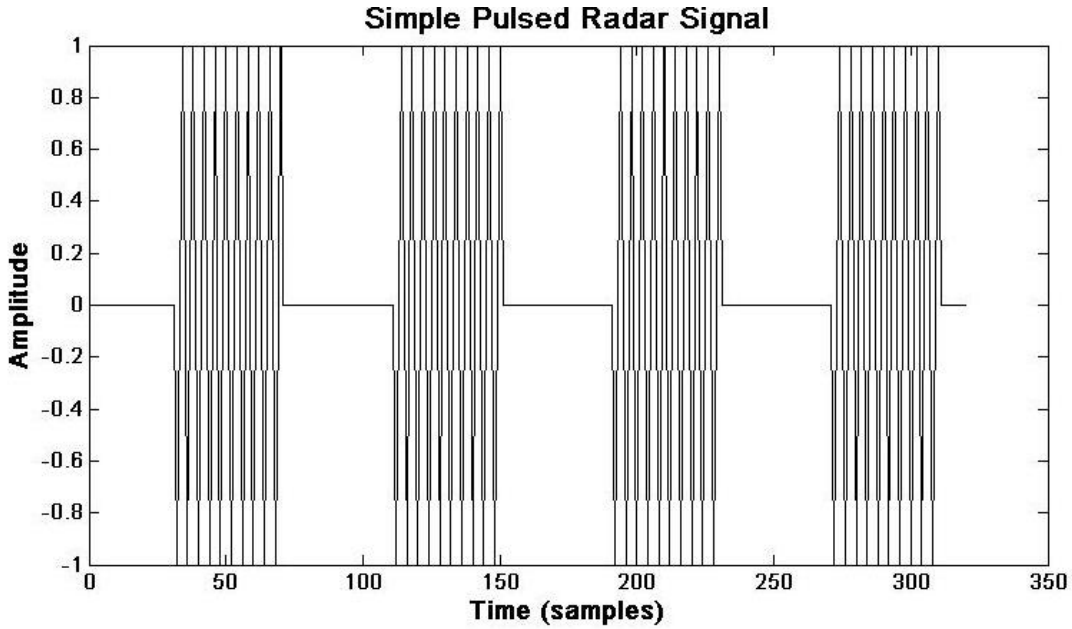

Fig. 1: Simple Pulsed Radar Signal

In Fig. 1, the signal is modulated sinusoidal within the PW duration and the waiting period for the return echo comes afterwards, the PRP is a combination of the PW and the waiting period. It is important to point out the Fig. 1 is presented as a form of illustration and in the practical world, the waiting period and hence the PRP is usually much longer than PW [10]. The theory behind the tools used in this paper are presented is subsequent subsections.

2.1. Short time Fourier transform

The STFT is the oldest, simplest and linear TFD which spurs from the classical Fourier transform. It uses sliding window to localize the content of the signal in a specific domain [11] or precisely, it is a process of splitting the time-domain radar signal into smaller segments and then the Fourier transform of each segment is evaluated [12]. The localization in one domain causes smear in the other domain due to the uncertainty principle, accounting for the major problem associated with this TFD [13]. This problem leads to optimization of usage or estimation of a domain trade-off when it is used. The STFT mathematically is given as:

$$S(t,f) = \int_{-\infty}^{\infty} s(\tau)w(\tau - t)\, e^{-j2\pi f\tau} d\tau \quad (1)$$

Where $s(\tau)$ is the signal, $w(\tau)$ is the window function used for the localization, whose Fourier transforms are given by $S(f)$ and $W(f)$ respectively. The magnitude version of the STFT is used in this work in order to counteract the unwanted imaginary values that comes about during the transformation, as such the more precise STFT used in the work is presented in equation (2);

$$S(t,f) = \left| \int_{-\infty}^{\infty} s(\tau)w(\tau - t)\, e^{-j2\pi f\tau} d\tau \right| \quad (2)$$

The window function $w(\tau)$ is used to break the signal into various segments in order to obtain the time-slice of signal so as to capture the spectral change. $w(\tau)$ is generally of positive values with concentration around zero value of time and frequency where maximum values are achieved. Due to the uncertainty principle, it is important that an optimal

window length is selected. Further discussion on this optimality is carried out in the upcoming section. The obtained three-dimensional (3D) time-frequency representation (TFR) is converted to a two-dimensional (2D) peak amplitude representation to cut down the processing burden of working with a 3D representation and design of simpler inter-pulse algorithm. The peak TFR of the STFT ($S(t,f)$) is given by;

$$S_{max}(t) = \max[S(t,f)] \tag{3}$$

This equation indicates S_{max} is gotten from the peaks range of the TFD from the frequency axis perspective of the T-F plane. Recently, the instantaneous frequency (IF) estimation which is based on the concept of S_{max} was used with the aid of other tools and theorem for signal analysis such as direction pattern [6] and Wiener-Khinchine and frequency law [8].

2.2. Window Functions

A window function is a restoring function that is used to truncate sample duration within a given interval. They have real, even and non-negative values equal to zero outside this interval and a non-zero value within the range of this chosen interval. If a window function is multiplied with another function, the product is also zero valued outside this chosen interval [14].
A variety of windows have been produced since the discovery of window functions for various applications. In the field of radar, they have been recently used for pulse compression radar processing [15], time delay estimation [16] and direction finding [17]. In this work, four basic and common windows are considered; Bartlett, Hanning, Hamming and Blackman. They all have significantly lower side lobes but higher main lobe width than the reference rectangular window when the window length is kept constant, providing a more smoothing operation [18] and hence localization in the T-F domain [11]. The summary of window functions used is given in table 1.

Table 1: Mathematical Representation of the Window Functions Used

Window	Equation (w(n)) Interval ($0 \leq \mathbf{n} \leq \mathbf{N}$)
Bartlett	$\mathbf{1 - {}^{2}/_{N}\left(n - {}^{N}/_{2}\right)}$
Hanning	$0.5^{-}0.5\mathbf{cos}\left({}^{2\pi n}/_{N}\right)$
Hamming	$\mathbf{0.54 - 0.46cos}\left({}^{2\pi n}/_{N}\right)$
Blackman	$\mathbf{0.42 - 0.5cos}\left({}^{2\pi n}/_{N}\right) + \mathbf{0.08cos}\left({}^{4\pi n}/_{N}\right)$.

The Bartlett window also known as the triangular window is formed from convolution of two rectangular windows, each of half duration. The Hamming and the Hanning (also known as Von hann) are basically the same window with the general formula as;

$$\alpha - (1-\alpha)\cos\left(\frac{2\pi n}{N} - 1\right) \tag{4}$$

Where α is a parameter that depends on the type of window in consideration. Furthermore, a graphical representation of window function used is presented in Fig. 2.

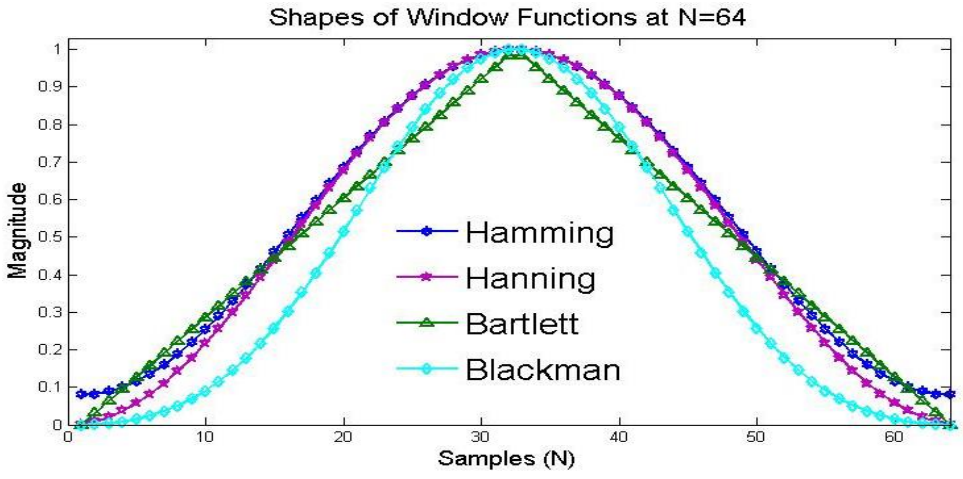

Fig. 2: Shapes of Window Function.

In Fig. 2, it is seen that there is a slight overlap between the Hanning and the Hamming windows, whereby the value of α is 0.5 for Hanning and 0.54 for Hamming. The slight increase in Hamming window was developed in order to effectively decrease its maximum side lobe amplitude, precisely reducing the ripple ratio by 50% [18]. The Blackman is similar to the Hanning and Hamming window with an additional cosine term as seen in Table 1 in order to reduce the ripple ratio but at the cost of increase in the main lobe width.

3. Methodology

Recent works have reported the use of different method for inter-pulse analysis. The novel PRP transform based on the concept of autocorrelation function was used to detect trains of jitter PRP configuration of up to 100 pulses [19] and an algorithm based on filters and fast Fourier transform (FFT) were used for PW and TOA estimation, achieving 100% probability of estimation at SNR of 4dB [20]. Most recently, the low-computationally complex smoothed instantaneous power was used for inter-pulse analysis of various types of radar signals with a 100 percent probability of estimation of 5dB in the worst case smoothing window irrespective of the incoming radar signals [21]. This paper provides an alternative inter-pulse algorithm based on STFT.

The algorithm presented in this paper is divided in two segments; T-F analysis and parameter estimation. The T-F analysis section deals with finding the STFT and subsequently its peak on the incoming signal. The parameter estimation section deals with extracting the PW and PRP from the peak plot obtained in the previous step. These segments are further explained in the subsequent sub-sections.

3.1. T-F analysis

The STFT is used to get the time-frequency representation (TFR) of the incoming radar signal using (2). An alternative mechanism based on selection of different STFT window function was created in this work in order to cater for the objectives of this paper. Also a small window length of 8 sample points was used in order to get an accurate time parameters estimation. It was found during a mini experiment that higher window length produces inaccurate time estimation especially when the effect of noise is considered due to the previously mentioned uncertainty principle between time and frequency. A contour plot of the obtained TFR of the incoming radar signal is shown in Fig. 3.

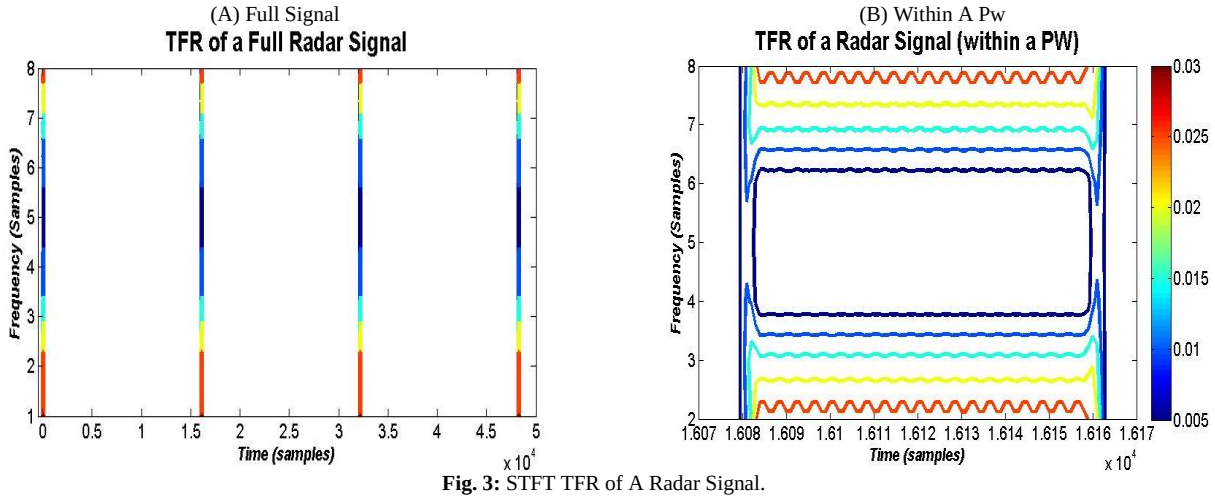

Fig. 3: STFT TFR of A Radar Signal.

The TFR of a full radar signal is shown in Fig 3a. Due to the always-longer PRP, Fig. 3b was plotted in order to show the TFR within the pulse width. The radar signal had a PW, PRP, centre frequency and sampling frequency of 1μs, 200μs, 10MHz and 80MHz respectively with Hanning window of 8 sample points was used in this illustration. Various colour codes represent different levels of amplitude and the bar at the left hand side provides a form of legend for these levels. It is seen in Fig 3b that a mirror is formed from the frequency axis perspective. This mirror is associated with the classical basic limitation of Fourier transform whereby non-required negative frequency mirror image of the signal is produced.

From Fig 3b, it can be seen by inspection using the colour bar that the maximum occur at a frequency sample point of 2. The other maximum at 8 is assumed to be the mirrored image and non-required. The equation for obtaining the equivalent centre frequency from a TFR representation is;

$$F_c = \frac{F_S}{TF_N} * (TF_F - 1) \quad (5)$$

Where F_c and F_s are the centre and sampling frequency respectively, while TF_N and TF_F are the T-F window length and T-F frequency point respectively. With a substitution of F_s=80MHz, and TF_N=8 and TF_F= 2 (obtained by inspection) in equation (5), a corresponding F_c of 10MHz is obtained hence confirming the original centre frequency of 10MHz, indicating that the TFR provides an accurate depiction of the incoming signal.
The peak of the STFT provides a form of conversion from the 3D TFR values to 2D peak values, hence allowing for a better and simpler algorithm to be designed. The corresponding peak plot obtained from the TFR in Fig. 3 using equation (3) is shown in Fig. 4;

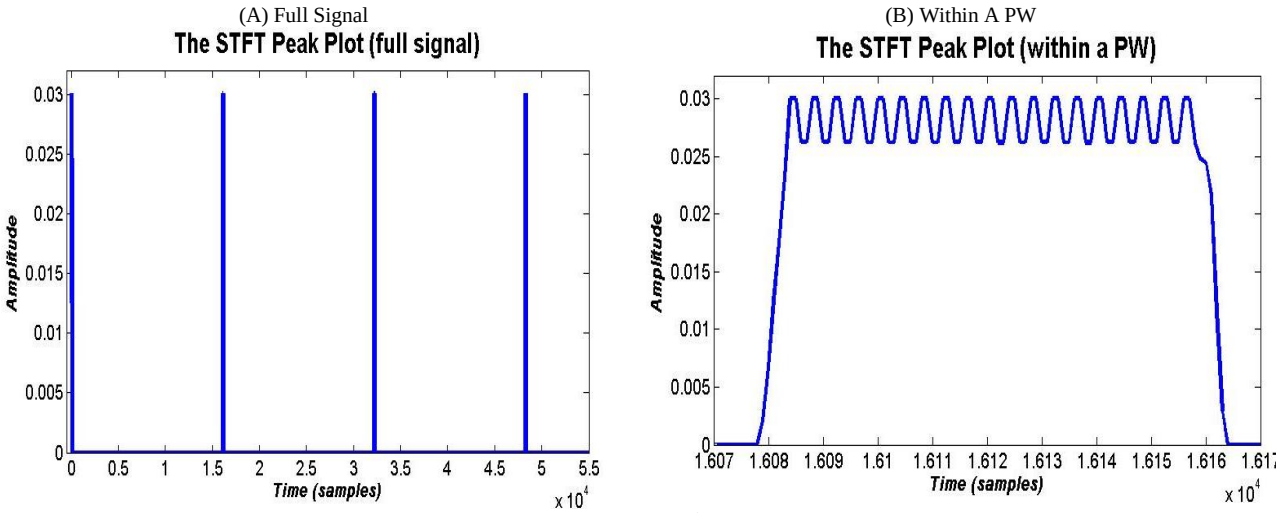

Fig. 4: The TFR Peak Plot of a Radar Signal

Fig 4a shows the TFR peak value of a radar signal while Fig 4b shows a magnified view of nature of this peak within a PW. It is seen that max value of 0.03 is achieved which corresponds to the maximum value obtained from colour-coded bar automatically generated as shown in Fig. 3. From the TFR peak value, an estimation algorithm is designed to estimate the PW and PRP, which is further explained in the next subsection.

3.2. Parameters estimation

In this section, two separate sub-algorithms are developed; one to estimate the PW and the other to estimate the PRP. In each case, the conventional approach of measuring the time parameters at half voltage point is used to counteract the effect of noise [3]. The voltage point is equivalent to the TFR peak obtained from the STFT. The half voltage is obtained by taking 50 percent of the max point of the TFR peak obtained. Thereafter, the obtained PW or PRP estimate is now converted from samples back to standard unit (seconds) using the sampling frequency. The equation for the conversion is given (6);

$$TP_{secs} = \frac{TP_{samples}}{f_s} \tag{6}$$

Where TP_{secs} is time parameter estimate in seconds, $TP_{samples}$is the time parameter estimated from the TFR peak in samples and f_s is the sampling frequency in Hz. Time parameter is either the PW or the PRP.

4. Results and discussion

The test reflected echo signal used in this work has a standard PW, PRP, centre frequency and sampling frequency of 1µs, 200µs, 10MHz and 80MHz respectively. The PRP value is selected such that the target emitter has an approximate unambiguous medium-range of 60km in free space. The noise considered for this work is the most common AWGN applicable to radar and communication systems. Ideally, it has a Gaussian probability density function, an impulse response autocorrelation and all frequency power spectra. The Monte Carlo simulation is used to investigate the performance of algorithm developed in the presence of uncertainty and variability within the signal-to-noise ratio (SNR) range of -6dB (low) to 14dB (high). SNR is obtained by (7);

$$SNR(dB) = 10\log_{10}\left(\frac{P_s}{P_n}\right) \tag{7}$$

Where P_s is the signal power and P_n is the noise power. Result obtained for the PW estimate using the Monte Carlo simulation of 100 runs at each SNR is presented in Fig. 5.

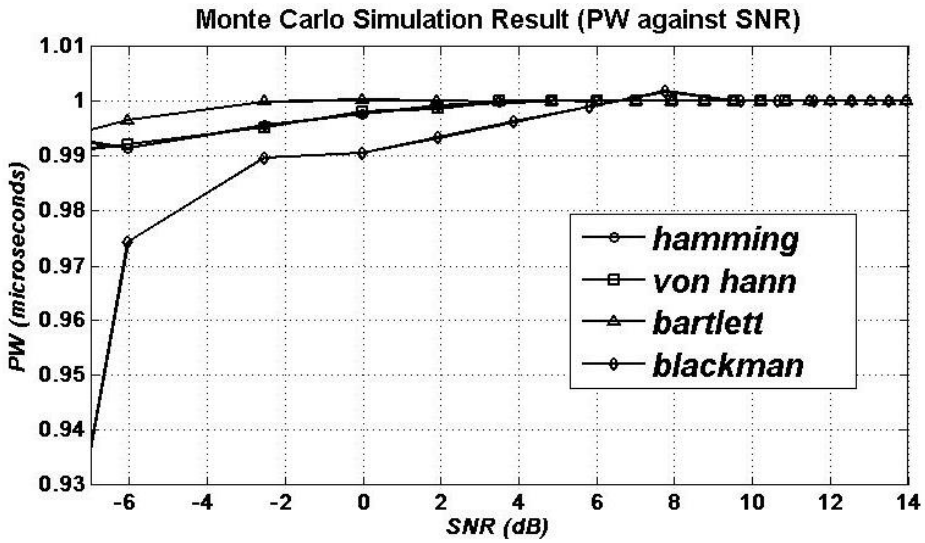

Fig. 5: PW Estimation Performance Result.

The result shows that Bartlett window performs best while the Blackman gave the least performance. Bartlett of highest peak side lobe when compared to other windows achieves a 100 percent accurate PW estimate at SNR of about -2dB, where the noise power is higher than the signal power. The rest of the windows require the signal power to be higher than the noise power in order to achieve the same feat. It is also seen that Hamming and Hanning has similar results as they share the same general equation (equation (4)) as there is only a slight increase in the α parameter. 100 percent PW estimation is achieved by both at SNR of about 4dB, and also the closeness in the results of Hamming and Hanning is seen in similar work where both windows where utilized [21].

The Blackman performs poorest as the extra cosine term as compared to the Hamming and Hanning windows increases the approximate transition of the main lobe width, achieving 100 percent estimate as SNR of 9dB. Also the Blackman window has lowest peak side lobe when compared to others. This discussion can be supported by an extract from [18] [22] presented in Table 2.

Table 2: Important Frequency Domain Characteristics of Some Window Function

Type of window	Approximate transition of the main lobe width	Peak side lobe (dB)
Bartlett	8π/N	-27
Hanning	8π/N	-32
Hamming	8π/N	-43
Blackman	12π/N	-58

Where N is the window length, Monte Carlo simulation was also carried out in order to examine the effect of windows on the PRP estimation using the STFT. Result obtained is presented in Fig. 6.

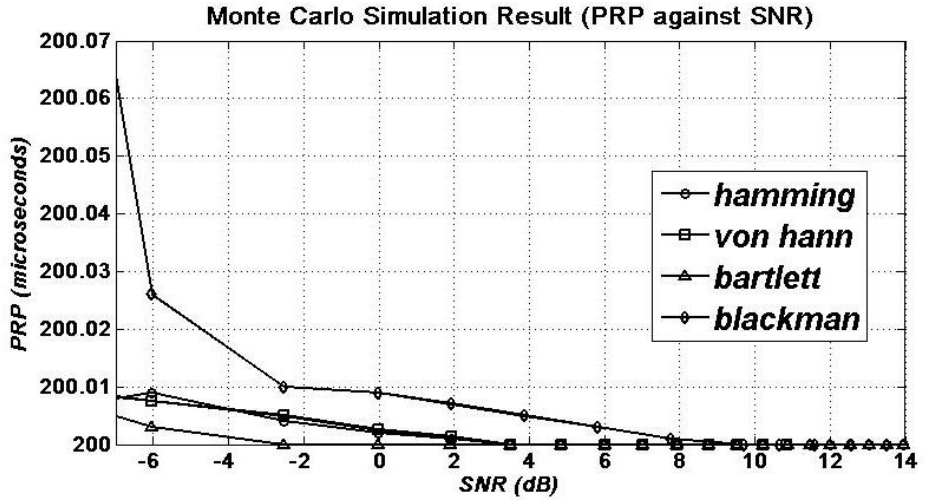

Fig. 6: PRP Estimation Performance Result.

It is seen in Fig. 6 that the SNR in which the windows achieves a 100 percent PRP estimation is similar to that of the PW estimate; about -2dB for Bartlett, 4dB for both Hanning and Hamming, and 9dB for Blackman. As such the effect of transition of the main lobe width and peak side lobe is the same as that of the PW estimate, and hence the previous discussion from the PW case is applicable to this result. The slight difference in both results is that error in PW estimate is actually negative before convergence to 100 percent estimate, while that of PRP estimate is positive. The setting of PRP threshold below the half voltage point causes a higher estimate when the effect of noise is present while that of PW is set at above the half voltage point and hence having a negative error result instead.
In general, determining whether the algorithm developed is better than previous inter-pulse algorithms [20] [21] will depend on the window function in consideration. The use of Bartlett window for the STFT analysis performs much better than previous similar works while the use of Hamming or Hanning produces no considerable improvement over previous works. The Blackman window-based STFT for inter-pulse analysis performs much poorer than previous work. It is also imperative to point out that the scope of this work is limited to a de-interleaved simple-pulsed radar signal and a standard of four sets of PRP configuration as given in [3].

5. Conclusion

This paper looks into an alternative inter-pulse analysis algorithm based on STFT, while jointly examining the effect of various window functions on the analysis using this TFD. It can be concluded that window functions of lower transition of main lobe width and higher peak side lobe performs best irrespective of the basic time parameter of the radar signal being estimated. As such, it is seen that the Bartlett (-2dB) performs best, then Hamming and Hanning window (both at 4dB) and finally Blackman window (9dB). From the result of inter-pulse analysis, further analyses such as intra-pulse analysis and signal classification can be carried out productively and objectively in order to meet an ELINT system objectives. The objective of future research work will be on interleaved and higher PRP configuration of radar signals.

References

[1] Adamy, D. L.; *EW101: A First Course in Electronic Warfare*, Artech House Inc., (2001).
[2] Adamy, D. L.; *EW102: A Second Course in Electronic Warfare*, Artech House Inc., (2006).
[3] Wiley, R. G.; *ELINT: The Interception and Analysis of Radar Signals*, Artech House Inc., (2006).
[4] Weihong, L., Yongshun, Z., Guo, Z., et al; 'A method for angle estimation using pulse width of target echo,' *International Conference on Wireless Communications & Signal Processing*, 2009. WCSP 2009, 13-15 Nov. (2009), pp.1-5, http://dx.doi.org/10.1109/WCSP.2009.5371635.
[5] Chen X., Guan, J., Bao Z., He, Y.; 'Detection and Extraction of Target With Micromotion in Spiky Sea Clutter Via Short-Time Fractional Fourier Transform', *IEEE Transactions on Geoscience and Remote Sensing*, Vol. 52, No.2,(2014), pp: 1002-1018, http://dx.doi.org/10.1109/TGRS.2013.2246574.
[6] Zhi-ren, C., Hong, G., Wei-min, S., et al; 'Micro-Doppler separation from Time Frequency Distribution based on direction pattern', *2014 12th International Conference on Signal Processing (ICSP)*, (2014), pp 2116- 2119. http://dx.doi.org/10.1109/ICOSP.2014.7015368.
[7] Tao, M ., Zhou, F., Liu, J. et al; 'Narrow-Band Interference Mitigation for SAR Using Independent Subspace Analysis', *IEEE Transactions on Geoscience and Remote Sensing*, Vol 52, No. 9, (2014), pp5289- 5301,. http://dx.doi.org/10.1109/TGRS.2013.2287900.
[8] Ahmad, A.A., Sha'ameri, A. Z.; 'Analysis and Classification of Airborne Radar Signal Types Using Time-Frequency Analysis,' *2014 International Conference on Computer and Communication Engineering (ICCCE)*, (2014), pp76-79, http://dx.doi.org/10.1109/ICCCE.2014.33.
[9] Skolnik, M.I.; *Radar Handbook*, Mc Graw-Hill Book Company, 3rd edn, (2008).
[10] Skolinik, M. I.; *Introduction to Radar Systems*, McGraw-Hill Book Company, 2nd Edn., (1980).
[11] Boashash,B.; *Time Frequency Signal Analysis and Processing: A Comprehensive Reference*, Elsevier, (2003).
[12] Chen, V.C., Ling, H.; *Time frequency transforms for radar imaging an signal analysis*, Artech House Inc., (2002).
[13] Gabor, D.; 'Theory of Communication', *Journal of the Institution of Electrical Engineering part III*, Vol. 93, No.26 ,(1946) , pp 429-457, http://dx.doi.org/10.1049/ji-3-2.1946.0076.
[14] Antoniou, A.; *Digital Signal Processing; Signal Systems and Filters*, Mc-Graw Hill Companies. Inc, 3rd edn, (2006)
[15] Escamilla-Hemandez, E., Ponomaryov, V.I.; 'Pulse compression radar processing based on atomic function windows' *The Fifth International Kharkov Symposium on Physics and Engineering of Microwaves, Millimeter, and Submillimeter Waves*, (2004). MSMW 04.,2, pp. 21-26, http://dx.doi.org/10.1109/MSMW.2004.1346242.
[16] Qu, L., Sun, Q., Yang, T., et al; 'Time-Delay Estimation for Ground Penetrating Radar Using ESPRIT With Improved Spatial Smoothing Technique,' *IEEE Geoscience and Remote Sensing Letter*, Vol. 11, No. 8, Aug (2014), pp.1315-1319, http://dx.doi.org/10.1109/LGRS.2013.2292825.
[17] Ramakrishnan, M., Ranjan, P.V.; 'Empirical Analysis of Energy Consumption in Wireless Sensor Networks,' *International Conference on Advances in Recent Technologies in Communication and Computing, 2009, ARTCom '09*, 27-28 Oct. (2009), pp.642-646, http://dx.doi.org/10.1109/ARTCom.2009.104.
[18] Proakis, J. G., Manolakis, D. G.; *Digital Signal Processing: Principles, Algorithm and Applications*', Prentice Hall, (1996)
[19] Nishiguchi, K., Kobayashi, M.; 'Improved algorithm for estimating pulse repetition intervals,' *IEEE Transactions on Aerospace and Electronic Systems*, Vol. 36, No. 2, (Apr 2000), pp.407-421, http://dx.doi.org/10.1109/7.845217.
[20] Wang, P. and Tang, B.; 'Detection and estimation of non-cooperative uniform pulse position modulated radar signals at low SNR, *2013 International Conference on Communications, Circuits and Systems (ICCCAS)*, 15-17 Nov. (2013), pp.214-217, http://dx.doi.org/10.1109/ICCCAS.2013.6765321.
[21] Adam, A. A., Adegboye, B. A. and Ademoh, I. A.; 'Inter-Pulse Analysis of Airborne Radar Signals using Smoothed Instantaneous Energy', *International Journal of Signal Processing Systems (IJSPS)*, ETPub, California, USA, in press.
[22] Lessard, C. S.; *Signal Processing of Random Physiological Signals*, Morgan & Claypool, (2006).